Evolution of Flaring Structures

Janusz Sylwester and Barbara Sylwester

Space Research Centre, Polish Academy of Sciences, Kopernika 11, 51-622 Wroclaw, Poland

Abstract. We present results of the study aimed to analyse the morphology of evolving coronal X-ray flaring structures. Our analysis deals with the Yohkoh SXT observations obtained during flares. In order to remove the telescope PSF blurring and improve the spatial resolution on the images we incorporated the ANDRIL maximum likelihood deconvolution algorithm. Using deconvolved images, we determined the distribution of physical conditions (Temperature-**T**, Emission Measure-**EM**) as they change with time for several flares. The results obtained indicate that the "magnetic connectivity" pattern is vividly changing as flare progress.

We put forward new "**hierarchical**" model of the coronal magnetic field organisation in order to explain the observed evolution of flaring structures.

1. Observations and Analysis

It is known, that appropriate numerical techniques may be used in order to remove the instrumental blurring from the measured images. This problem has been considered in detail in relation with known troubles of Hubble Space Telescope mirror (White et al., 1993, 1994). We present results of application of the maximum likelihood method of image enhancement to the interpretation of soft X-ray images obtained by SXT telescope aboard the Yohkoh Japanese solar satellite. Applied deconvolution procedure (ANDRIL) provides X-ray images with angular resolution below 1 arcsec as taken in different energy bands. These deconvolved images have been analysed in order to derive maps of distribution of basic physical characteristics of flaring plasma. In the present study we analyse flares observed close to the limb since it is easier to distinguish in this case the vertical stratification of the X-ray emission. As described in more detail by Sylwester at al., (1996), we deconvolved the instrumental point spread function (PSF) from the original images recorded by SXT. As the PSF shape depends substantially on the position of the source within telescope field of view, we have used approximate formulae derived by Martens et al., (1995). In the deconvolution, we divided each of the original 2.45 arcsec $\times$ 2.45 arcsec CCD pixel into 25 sub-pixels increasing in this way the spatial resolution. However, this increase in resolution causes sometimes problem with an artificial "noise" showing up on deconvolved images taken with short exposures. The problem occurs in areas where signal level is of the order of dark current (out of bright flare kernels). Such "noise" may lead to unreasonable values of derived parameters. We discuss later, how to avoid this problem, at least partly. In Fig. 1, we show sequence of deconvolved images obtained through Be119 filter for 11 August 1992 flare. One may recognize there the presence of white patches corresponding to these "noisy" regions. In order to lessen the "noise" problem, we decided to

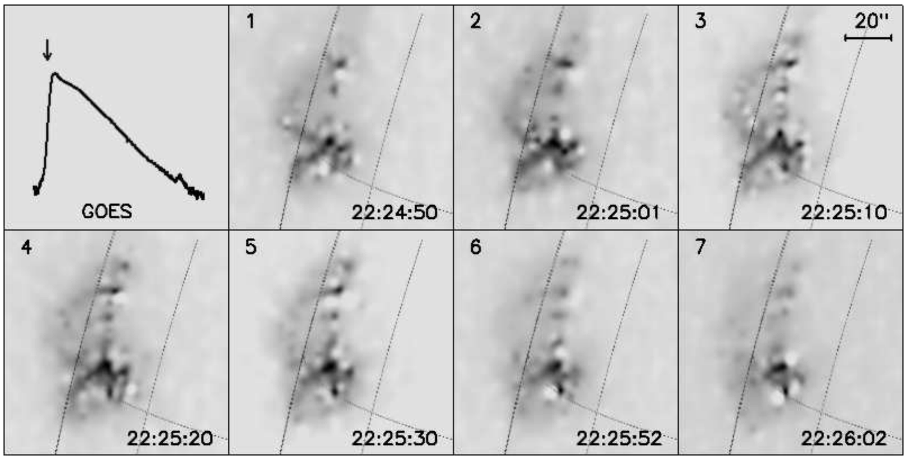

Figure 1. Example initial sequence of seven consecutive deconvolved Be119 frames for 11 August 1992 flare. The frames have been coaligned to within one sub-pixel (0.5 arcsec) using the satellite pointing data. The frame cadence is $\sim$ 10 s. In the upper left corner, GOES plot for the corresponding flare is shown with the arrow pointing to the time when selected frames have been obtained. Dotted lines (here and in the other figures) correspond to the heliocentric coordinate system with the leftmost one representing solar limb. The intensity scaling (individual for each image) is very flat (power $\sim 1/5$) in order to bring up weak structures.

add (weighting by exposure time) several (usually five) consecutive deconvolved images obtained using particular filter. We coaligned the images according to the Yohkoh satellite pointing file to within one sub-pixel. This summed picture represents the average deconvolved image (over time interval of several tens of seconds). The frames getting into the sum we selected in such way, that the mean times corresponding to Be119 and Al12 images differ by no more than few seconds and therefore the analysis of their ratio is meaningful. As pointed out by Siarkowski et. al., (1996), the determination of emission measure and temperature maps from image ratios constitutes a "delicate" task, especially in case of the SXT measurements where the satellite axis had been pointing in slightly different directions between exposures. It has been shown in that paper that the most important is precise alignment of images to within fractions of arcsec. The satellite pointing data are usually not that accurate and additional pointing corrections are necessary. Appropriate alignment is even more important when *deconvolved* images are to be compared because of the smaller size of the sub-pixel. Therefore, before deriving **EM** and **T** maps, we coaligned precisely Be119 and Al12 images using multiplicative method (for details see Siarkowski et. al., 1996). Usually the applied additional shifts are of the order of fractions of arcsec. Ratios of Be119/Al12 signals we have interpreted using standard isothermal approximation and as a result two characteristic parameters (**T**, **EM**) have been derived for each sub-pixel. In Fig. 2 and 3 we present sequences of high-resolution maps of emission measure for two limb flares. The

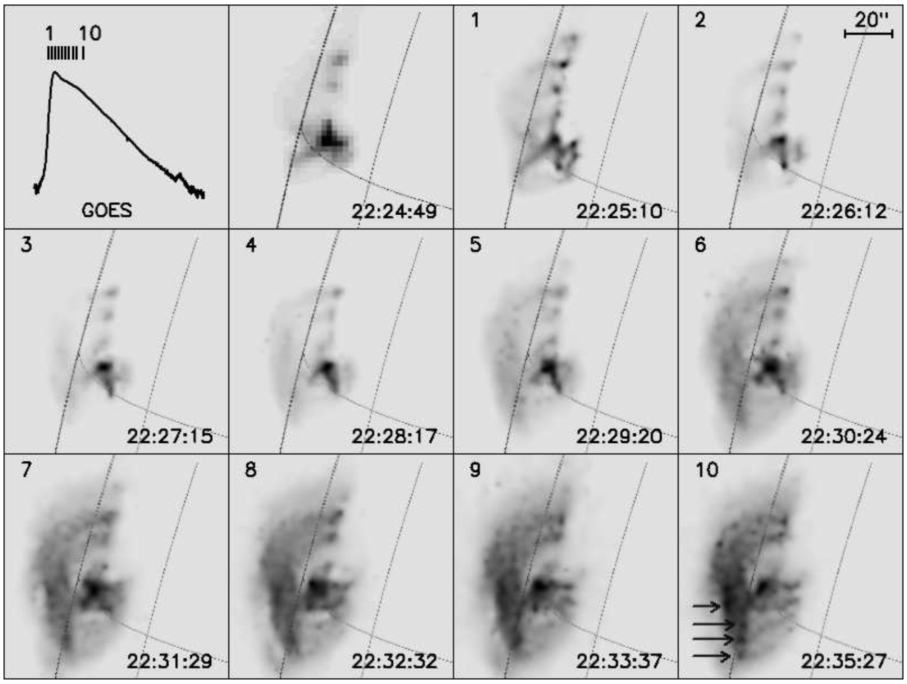

Figure 2. The sequence of ten emission measure maps for 11 August 1992 flare. The frames have been precisely coaligned as discussed in the text. The scaling of images is again very flat. The frame next to GOES represents pre-flare situation as seen on the original Be119 image.

important result of described analysis procedure is that the "noise" problem is mostly removed. It comes out that the detailed morphology of X-ray sub-arcsec flare structure is richer, smoother and more detailed on the emission measure map as compared to that seen on summed image obtained from a given filter. In the present paper we investigate evolution of flare morphology basing on the emission measure maps. Discussion of behaviour of the temperature for selected kernels is given in a parallel research by B. Sylwester and J. Sylwester (1998).

2. Results

We have analysed the evolution of deconvolved high-resolution intensity maps and emission measure distributions using time-lap animation. There are number of conclusions coming out from such analysis as concerns several limb flares investigated:

- As a rule, a number of bright X-ray patches are present at the places where extended coronal structures are rooted. These patches are contributing the most to the soft X-rays during the rise phase.

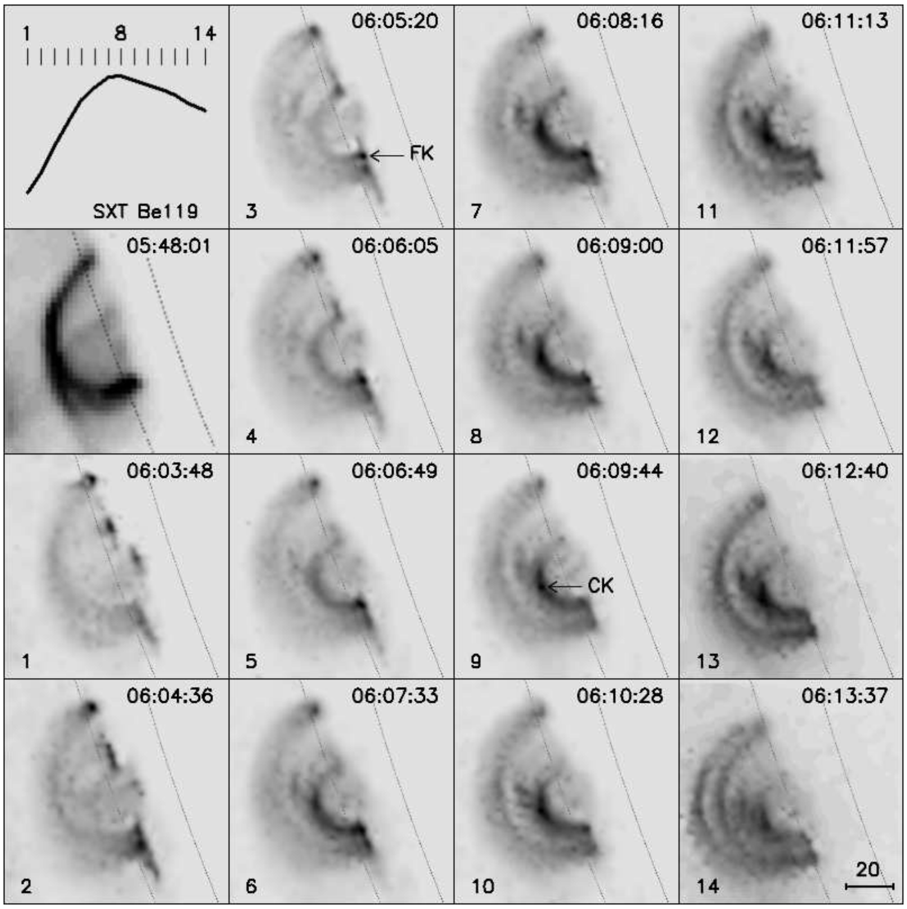

Figure 3. The same as in Fig. 2 for 30 November 1993 flare, except that instead of GOES (unavailable), the integrated (over the frame area) time variation of the Be119 flux is plotted. Arrows point to the kernels (FK, CK) for which physical conditions have been analysed by B. Sylwester and J. Sylwester, (1998).

- The morphology of foot-point patches closely resembles arcades of compact low lying loops with the length of $10^4 - 5 \times 10^4$ km and the perpendicular size of $3000 - 5000$ km. We call these regions foot-point arcades (FA).

- The roots of coronal loops "move" (jump) along the FA as flare progress. Velocity of this "motion" can reach $20 - 30$ km/s. Such "motions" are typical. It is quite unusual (we never identified such a case) to see particular foot-point kernel to be bright throughout the entire flare at the same place. However, foot-point kernels are present also during flare decay.

- Sometimes, there are seen low lying "ridges" (backbones) joining near-by FA (cf. Figs 1 and 2). Fast rearrangement of morphology of these ridges is typically observed during rise phase. Particular FA are connected by reorganising patches of emission at different times. The rearrangement of the "graph" connection pattern can be so fast that some of its behaviour may be overlooked on images taken even seconds apart (cf. Fig. 1).

- It is typical to observe substantial changes in the morphology of the upper flaring coronal structures between the rise and decay phases. Dominating coronal kernels can be easily distinguished. They brighten and decay in several locations as flare evolves. It is very suggestive that elongated loops extending higher into the corona merge at (originate from) these bright kernels (cf. arrows in the frame No. 10 in Fig. 2).
- For all investigated flares the initial and the final magnetic "connectivity pattern" is different. For certain flares it is possible to follow smooth changes of this pattern as flare evolves. However sometimes the evolution resembles lightnings. We have noticed that rearrangement of the connectivity pattern is related to motions of the loop "root-points" along the low-lying ridges joining individual FA and/or coronal kernels.

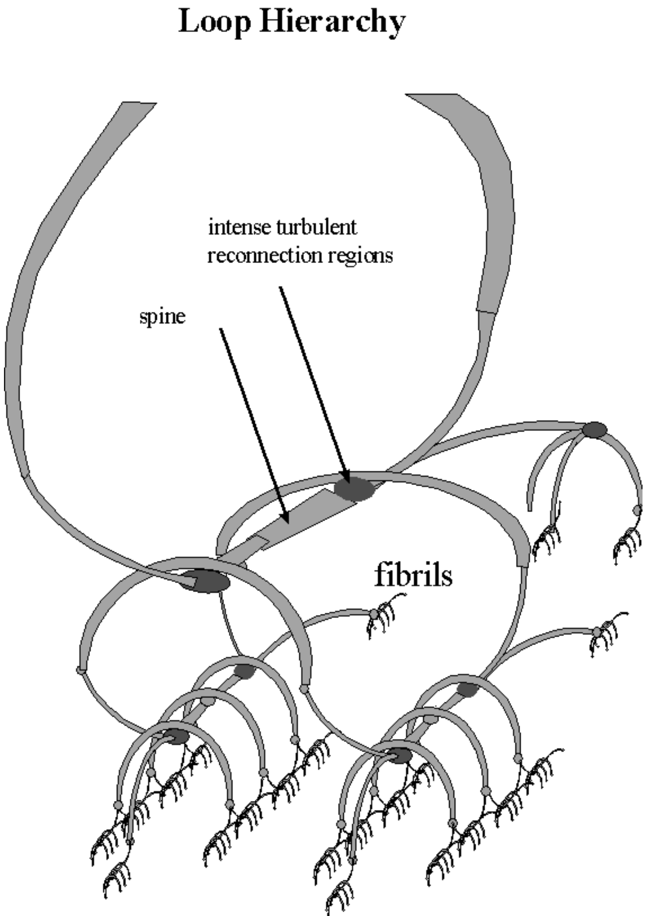

Figure 4. Proposed hypothetical loop hierarchy structure of magnetic fields in the corona.

As a result of the analysis of these observations we came to the conclusion that classical "magnetic connectivity" pattern, with foot-points of the coronal loops "permanently anchored" to particular magnetic flux tube emerging from below the photosphere does not fit to the above findings. It seems necessary to reconsider this "classical" point of view.

Based on the present morphological study, we introduce a new "cartoon" of connectivity pattern for the field lines in the corona. This cartoon is shown in Fig. 4. We call it the "hierarchical model". In this model we postulate the existence of a hierarchy of loop systems in which larger loops are rooted somewhere at the ridges joining tops of low-lying arcades connecting the opposite magnetic polarities. This low-lying arcades, perhaps, yet again, follow this organisation on even smaller scales (fractal structures?). The ultimate smallest flux-tubes seem to be those which emerge from below the photosphere as the ephemeral regions within the plage domain of one dominant polarity. Such a picture may get support from the NIXT observations (Golub at al., 1990; Herant et al., 1991) where compact X-ray loops are observed within the particular Hα ribbon. The uppermost loop systems related to active region and/or the complex of active regions (possibly showing up as coronal helmet structures) are tighted up by solar wind. During the flare (or micro- or nanoflare), through the process of reconnection of magnetic field lines inside multiple turbulent reconnection kernels (cf. Jakimiec at al., 1998), the overall magnetic field pattern simplifies causing stepwise relaxation of the magnetic surplus energy.

Acknowledgments. We are grateful to Mrs. A. Kepa for preparing videos and figures related to this research. This work has been supported by a KBN Grant 2.P03D.006.10 of Polish Committee for Scientific Research.

References

Golub, L., Herrant, M., Kalata, K., Lovas, I., Nystrom, G., Pardo, F., Spiller, E. & Wilczynski, J. 1990, Nature, 344, 842

Herant, M., Pardo, F., Spiller, E. & Golub, L. 1991, ApJ, 376, 797

Jakimiec, J., Tomczak, M., Falewicz, R., Phillips, K.J.H. & Fludra, A. 1998, A&A, submitted

Martens, P. C., Lemen, J. R. & Acton, L. W. 1995, Solar Phys., 157, 141

Siarkowski, M., Sylwester, J., Jakimiec, J. & Tomczak, M. 1996, Acta Astronomica, 46, 15

Sylwester, J., Sylwester, B. & Siarkowski, M. 1996, PASP, Magnetic Reconnection in the Solar Atmosphere, ed. R.D. Bentley & J.T. Mariska, 244

Sylwester, B. & Sylwester, J. 1998, JOSO Annual Report 1997, submitted

White, R. L. 1993, STS Image Reconstruction Newsletter, 11

White, R. L. 1994, Restoration of HST Images and Spectra II, 104